An elasto-viscoplastic finite element study of the effect of footing roughness on the failure mechanism and bearing capacity of inhomogeneous clay deposit

Kyoto University	Student member	○ B. Siribumrungwong
Kyoto University	Fellow	F. Oka
Kyoto University	Member	T. Kodaka
Kyoto University	Member	S. Kimoto
Kyoto University	Member	Y. Higo

1. Introduction

By plasticity solution, frictional condition at footing surface affects the failure mechanism but have no effect on the bearing capacity for footing on soil with constant undrained shear strength. However, in the case of strip footing on clays of undrained shear strength increasing with depth, change of the failure mechanism associated with different frictional condition will significantly affect the bearing capacity (Davis and Booker (1973)) and therefore, must be included in the analysis. In the present study, the finite element analysis of bearing capacity of surface foundation on clay which is inhomogeneous only in the vertical direction is conducted using an elasto-viscoplastic soil constitutive model considering microstructure change. A series of analysis of footings on inhomogeneous clay deposit with different footing roughness conditions have been carried out. The effects of microstructure change and strain localization on the bearing behavior are also discussed in the study.

2. Elasto-viscoplastic constitutive model for clay considering microstructure change

An elasto-viscoplastic soil constitutive model for both NC and OC clays considering microstructure change proposed by Kimoto (2002) is adopted in the numerical analysis. The model is based on the Cam clay model and Perzyna type of viscoplasticity theory. The model can describe the rate dependent behavior, such as the acceleration creep failure and the dilatancy characteristics. In this model, total strain rate can be obtained from Equation (1) and viscopalstic strain rate is given by Equation (2).

$\dot{\varepsilon}_{ij} = \dot{\varepsilon}^{e}_{ij} + \dot{\varepsilon}^{vp}_{ij}$ (1), $\dot{\varepsilon}^{vp}_{ij} = \gamma \left\langle \Phi_1(f_y) \right\rangle \dfrac{\partial f_p}{\partial \sigma'_{ij}}$ (2), $\dot{\varepsilon}_{ij}$: Total strain rate tensor, $\dot{\varepsilon}^{e}_{ij}$: Elastic strain rate tensor, $\dot{\varepsilon}^{vp}_{ij}$: Viscoplastic strain rate tensor, f_y: Static yield function, f_p: Plastic potential, Φ_1: Material function indicating strain rate sensitivity. In order to describe the degradation of the material caused by structural changes, diminution in size of f_y and f_p with the viscoplastic strain is incorporated by introducing two independent parameters, β and σ'_{maf} into the constitutive equation. β is the parameter which denotes the degradation rate of the material strength and σ'_{maf} provides the degree for a possible collapse of the structural at the initial state.

3. Numerical simulation

Numerical simulations under plane strain conditions have been carried out by the finite element method using the updated Lagrangian method with the objective Jaumann rate of Cauchy stress for a weak form of the equilibrium equation. Biot type of two-phase mixture theory (Biot, 1956) is used with a velocity-pore pressure formulation. An eight-noded quadrilateral element with a reduced Gaussian (2x2) integration is adopted in the analysis. The pore water pressures are defined at four corner nodes. Figure 1 shows the geometry of problem analyzed. Distribution of soil initial stress as well as the peak and residual shear strength obtained from one element simulation are shown in figure 2. Table 1 shows the parameters of NC clay used in the analysis. The footing displacement rate is 2.0x10^{-4}m/min. A series of analysis using different footing roughness condition and β value is carried out in order to study their effects on the failure mechanism and the bearing capacity.

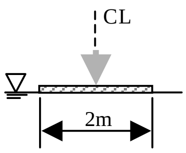

Figure 1: Loading Condition for the analysis

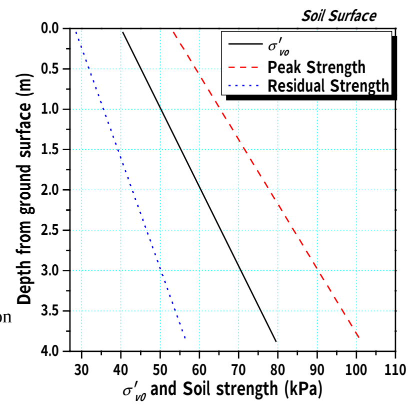

Figure 2: Profile of initial stress and undrained shear strength

Key word　Bearing capacity, Elasto-viscoplasticity, Microstructure change, Inhomogeneity

Contact address　606-8501 京都市左京区吉田本町　京都大学大学院工学研究科社会基盤工学専攻地盤力学分野　TEL　075-753-5086

4. Results and discussion

Table 1: Soil parameters

k_0 (m/s)	$0.8\mathrm{x}10^{-9}$
$G_0/\ \sigma'_{m0}{}^{1/2}$	1307
λ	0.508
κ	0.0261
e_0	1.70
K_0	1.0
M^*_m	1.09
m'	18.5
C_0 (1/s)	$1.3\mathrm{x}10^{-13}$
$\sigma'_{maf}/\ \sigma'_{mbi}$	0.517
β	0, 20

As can be seen in figure 3, Prandtl's failure mechanism is predicted for the rough footing while the smooth footing gives Hill's failure mechanism. Figure 5 shows the comparison between the total reaction forces at the footing surface. The bearing capacity for the smooth footing is lower than that for the rough footing. This occurs because the horizontal restraint imposed at the soil-footing interface causes the failure mechanism to penetrate deeper into the soil for the rough footing case. As the undrained shear strength increases with depth, this causes the higher bearing capacity for the rough footing than for the smooth footing. Distribution of accumulated viscoplastic shear strain for the case of footing with coefficient of friction μ=0.1 and 0.2 are also shown in the figure 3. The failure mechanisms obtained from these cases can be considered as the intermediate failure mechanism for the rough and smooth footing and therefore show the transition between the Prandtl and Hill failure mechanism. Consequently, the bearing capacity obtained from the frictional footing is between that of the smooth footing and the rough footing. Peak shear strength obtained from one element simulation shown in figure 2 and the peak reaction forces from high structured soil (β=20) shown in figure 5 have been used to calculate bearing capacity factor N_c. The calculation yields N_c of 5.22 and 5.45 for smooth and rough footing respectively. The obtained valued is considerably lower than that from plasticity solution proposed by Davis and Booker (1973), which yields N_c of 5.48 and 5.85 for the soil profile used in this study. Such behavior is caused by the degradation of soil strength simulated in the analysis. For the high structured soil (β=20), strain localization is clearly predicted. With displacement of the footing, total reaction force obtained from the highly structured soil will rise to the peak value, then drop gradually to residual value and remain constant with further displacement. This is because the degradation of soil strength and strain localization. On the other hand, by the lack of strain localization and structure degradation, figure 4 shows that pushing the footing deeper into the soil will shear the soil that located at deeper position and makes the reaction force at footing on low structured soil continue to increase, and neither peak nor residual value is observed. Since the strength and stiffness of soil increase with depth, the gradient of increases of reaction force in this case is considerably high. As shown in figure 5, reaction force for the rough footing on low structured soil obtained at 12cm of footing displacement is almost 20% higher than the reaction force obtained at 2cm of footing displacement.

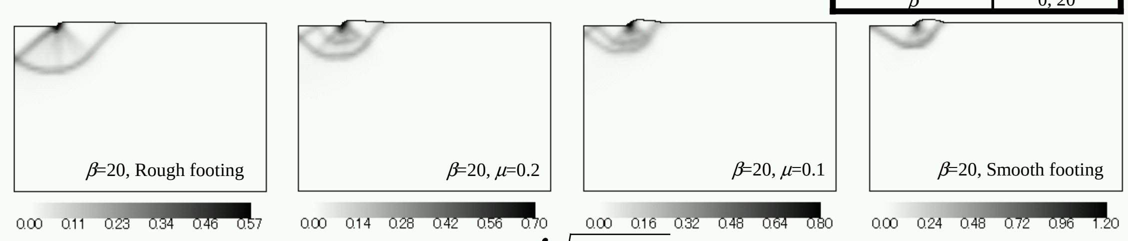

Figure 3: Distribution of viscoplastic deviatoric strain $\left(\gamma^p \equiv \int \sqrt{de^{vp}_{ij}\, de^{vp}_{ij}}\right)$ from high structured soil at 6cm of footing displacement

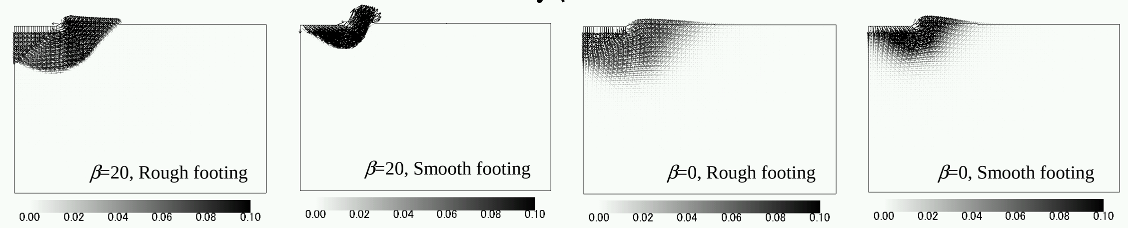

Figure 4: Vectors of incremental displacements

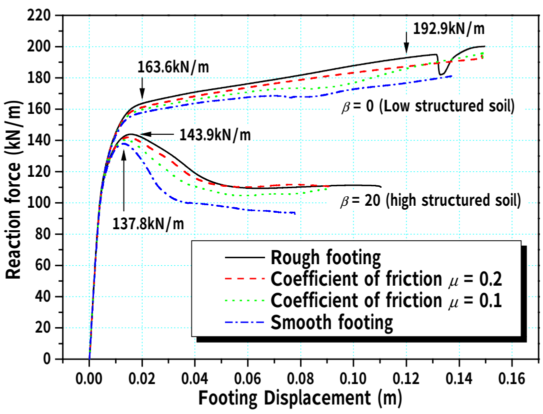

Figure 5: Load-displacement curves for strip footing

5. Conclusion: Friction conditions at footing surface affect the failure mechanism and consequently result in different bearing capacity. Soil strength degradation and strain localization due to the collapse of soil structure affect the bearing behavior of the footing. For the clays of undrained shear strength increasing with depth, by the lack of strain localization, the gradient of increasing of reaction force in the case of low structured soil is considerably high.

6. **Reference:** 1) Davis, E. H., and Booker, J.R., Geotechnique, Vol.18(1), pp.67-91, 1973. 2) Kimoto, S., Doctoral thesis, Kyoto university, 2002. 3) Oka, F., Higo, Y. and Kimoto, S., International Journal of Solids and Structures, Vol.39, pp.3625-3647, 2002.